Estonian Journal of Earth Sciences
2025, **74**, 2, 83–95

https://doi.org/10.3176/earth.2025.06

www.eap.ee/earthsciences
Estonian Academy Publishers

RESEARCH ARTICLE

Received 8 October 2024
Accepted 26 November 2024
Available online 8 March 2025

Keywords:
Earth science, palaeoclimatology, dendrochronology, phenology, Finland, Holocene

Corresponding author:
Samuli Helama
samuli.helama@luke.fi

Citation:
Helama, S., Holopainen, J., Fuentes, M., Rocha, E. and Gunnarson, B. E. 2025. Boreal temperature variability inferred from latewood maximum density and historical plant phenology records. *Estonian Journal of Earth Sciences*, **74**(2), 83–95. https://doi.org/10.3176/earth.2025.06

Boreal temperature variability inferred from latewood maximum density and historical plant phenology records

Samuli Helama[a], Jari Holopainen[b], Mauricio Fuentes[c], Eva Rocha[d] and Björn E. Gunnarson[e,f]

[a] Natural Resources Institute Finland, Ounasjoentie 6, 96200 Rovaniemi, Finland

[b] Natural Resources Institute Finland, Latokartanonkaari 9, 00790 Helsinki, Finland

[c] Gothenburg University Laboratory for Dendrochronology (GULD), Regional Climate Group, Department of Earth Sciences, University of Gothenburg, Medicinaregatan 7B, 41390 Gothenburg, Sweden

[d] UMR 7209, Muséum national d'Histoire naturelle, BioArchéologie, Interactions Sociétés environnements, CP56, 55 rue Buffon, 75005 Paris, France

[e] Department of Physical Geography, Stockholm University, Svante Arrhenius väg 8, 10691 Stockholm, Sweden

[f] Bolin Centre for Climate Research, Stockholm University, Svante Arrhenius väg 8, 10691 Stockholm, Sweden

ABSTRACT

Plant-based data from southern Finland were used to reconstruct late Holocene warm-season temperature variability on inter-annual to longer scales. Temperature-sensitive records representing maximum latewood density of *Pinus sylvestris* tree rings (since AD 760) and phenological stages of several plant species (since AD 1750) explained ~60% and ~70% of instrumentally observed temperature variance, respectively. The value of a multi-proxy approach was demonstrated by statistical models including both variables, which explained ~80% of the temperature variance. Temperatures from the CRUTEM5 and Berkeley datasets had slight variations in their correlativity with proxy data, possibly resulting from their differing spatial representativeness over the proxy sites. Temperature history inferred from maximum latewood densities extended over the past millennium and correlated with previously published data from similar proxy records in Fennoscandia and adjacent areas. These data indicate that the region cooled since the Medieval Climate Anomaly and warmed markedly since the Little Ice Age/Maunder Minimum. In the study region, the magnitude of this long-term warming was 2.1 °C and 2.8 °C, calculated between the coldest and warmest 100-year and 30-year intervals, respectively. Collectively, our results display the potential of plant-based data from low-lying and mild boreal sites to extend our understanding of preindustrial and recent climatic changes.

Introduction

High-resolution temperature reconstructions are needed to expand our understanding of past and present climatic events. Tree rings are frequently used to reconstruct climate variability on seasonal to longer timescales. Among tree-ring variables, maximum latewood density (MXD) data show markedly strong and consistent correlations with warm-season temperatures (Briffa et al. 2002a, 2002b), and MXD-based late Holocene temperature reconstructions have been developed in the extratropical Northern Hemisphere to expand knowledge of climate variability prior to the instrumental and industrial periods (Wilson et al. 2016; Anchukaitis et al. 2017). Another high-resolution, indirect (i.e. proxy) source of climate data is provided by historical documents, especially phenological observations (Kington 1974). Valuable sources of quantitative climate data have been produced for various sites with a rich availability of historical observations on plant phenological stages, such as flowering and harvest dates (Tarand and Kuiv 1994; Tarand and Nordli 2001; Chuine et al. 2004; Aono and Kazui 2008; Zheng et al. 2015; Aono and Nishitani 2022).

The objective of this study was to build quantitative temperature reconstructions from MXD and plant phenological records for low-lying areas in the southern part of Finland (below ~65° N). Similar records have previously been used for late

Holocene temperature reconstructions in the same region (Holopainen et al. 2006, 2009; Helama et al. 2014b); however, our study is augmented by new data that substantially increase the sample depth of both tree-ring and phenological observations, with updates to the previously explored records. These data include the recently compiled plant phenological dataset collated from historical observations, available since AD 1750 (Holopainen et al. 2023a), as well as our hitherto unpublished MXD records from subfossil and living-tree samples that cover the time frame of the past eight centuries. To our knowledge, no previous studies have combined tree-ring and phenological records to reconstruct past climate variability in this or nearby regions.

Our aim contrasts with several previous studies focusing on MXD archives from high-latitude and high-altitude sites in Fennoscandia, including northern Finland (for a review of past literature, see Linderholm et al. 2010). Our low-lying sites in southern Finland represent a mild boreal climate zone, where plant activity may be less responsive to warm-season temperatures, according to classical examples (e.g. Fritts 1976; Babst et al. 2013), in comparison to their northern and alpine counterparts. Even so, the scarcity of high-resolution reconstructions from such mild sites necessitates the development of new data and novel approaches also for these regions, where correlations between proxy and instrumental climate records may be suboptimal.

Two specific hypotheses were tested: (1) that the ongoing warming recorded in the study region (Tietäväinen et al. 2010; Irannezhad et al. 2015; Mikkonen et al. 2015) has resulted in an exceptional warming event in the context of late Holocene temperature reconstructions; (2) that the value of multiple proxy records (Mann 2002) is manifested with evidence of more reliable reconstructions when both the MXD and phenological records, rather than either one alone, are included as variables in the statistical models explaining the instrumentally observed warm-season temperatures. Our MXD record was also compared with similar (near-)millennial tree-ring records from Fennoscandia (Wilson et al. 2016). Collectively, our analysis presents a proxy/climate assessment and an evaluation of late Holocene temperature histories, focusing on sites that have been too long neglected in the palaeoclimate literature.

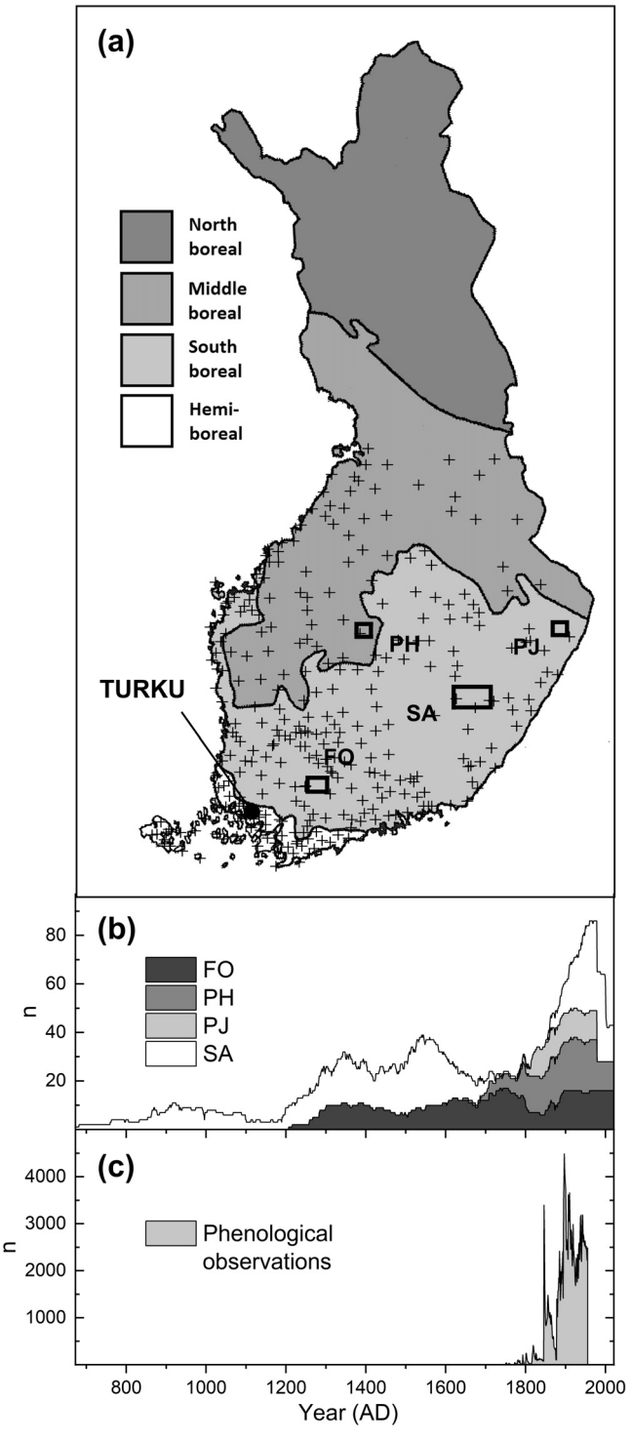

Fig. 1. Geographical and temporal coverage of the site chronologies. **(a)** Map of Finland showing the locations of the studied tree-ring chronologies in the region of Forssa (FO) and Savonlinna (SA), and in the national parks of Pyhä-Häkki (PH) and Petkeljärvi (PJ), in relation to the vegetation zones (redrawn after Virkkala et al. 2000). Crosses mark the sites where phenological observations have been made (a limited number of sites outside the terrain of today's Finland are not shown). The site of Turku, where early meteorological observations were made, is also indicated. **(b)** Temporal variations in the replication of maximum latewood density records from the FO, PH, PJ, and SA sites. **(c)** Temporal variations in the number of phenological observations per year.

Materials and methods

New MXD data

New tree-ring materials were collected from Forssa (FO), Pyhä-Häkki (PH), and Savonlinna (SA) sites (Fig. 1; Table S1). Tree-ring samples were extracted from living Scots pine (*Pinus sylvestris* L.) trees using an increment borer (Ø = 10 mm) approximately 130 cm above the root collar, with one sample per tree, in late autumn/early winter in 2021. The forests in this area belong to the south and middle

boreal zones (Ahti et al. 1968), situated roughly between 75 and 185 metres above sea level. The FO and SA sites represent riparian habitats of small lakes, whereas the trees from the PH site originate from an upland habitat in a national park (Virkkala et al. 2000; Lappalainen 2001). Permissions for tree-ring sampling were obtained from landowners and the state forestry administration to allow the fieldwork. Collected materials were analysed using standard dendrochronological routines (Fritts 1976; Speer 2010). The widths of consecutive tree rings were measured under a light microscope to the nearest 0.01 mm. Tree rings were cross-dated both statistically (Holmes 1983; Helama 2023) and visually by comparing the resulting ring-width graphs with each other and against existing master chronologies (Helama et al. 2005, 2014a, 2024). Moreover, subfossil tree-ring samples of the FO site, originally retrieved from the lake sediments of Lake Kaitajärvi and Lake Vähä-Melkutin, were obtained for the purpose of this study. These samples have been cross-dated and shown to cover a period of the past eight centuries (Helama et al. 2014a).

MXD data were produced using X-ray-based microdensitometry, following the protocols described by Gunnarson et al. (2011). Samples were sawn into thin laths (1.2 mm thick) using a twin-bladed circular saw, treated with alcohol in a Soxhlet apparatus to remove extractives unrelated to wood density (Schweingruber et al. 1978), and acclimatised to 12% moisture content (air dry). An ITRAX Wood Scanner from Cox Analytical Systems (Sweden), equipped with a chrome tube tuned to 30 kV and 50 mA, was used to produce high-resolution radiographic images. Mounted samples were exposed to a narrow, high-energy X-ray beam in 20 µm steps, with a 75 ms step time. For each step, a sensor with a slit opening of 20 µm registered the radiation not absorbed by the sample. Eight-bit, greyscale digital images were produced with a resolution of 2540 dpi, the grey levels being calibrated using a calibration wedge from Walesch Electronic (Switzerland). The images were evaluated using WinDENDRO tree-ring image processing software from Regent Instruments (Canada), which provides ring-width and density data from a scanned image (Guay et al. 1992). Density profiles from the pith towards the bark were obtained through the lines, avoiding hollow and rotten parts of the samples. Ring widths measured under the microscope and from the software were matched to assign calendar years to the MXD data.

Previously produced MXD data

The new density data were combined (see the next section for methods) with previously published MXD data from the SA site (Helama et al. 2008, 2010, 2012, 2014b). This set of samples represents subfossil and living *Pinus sylvestris* trees, forming an MXD chronology spanning roughly the past thirteen centuries (Table S1). In addition to the foregoing papers, the microdensitometric methods used to produce the data have been described by Peltola et al. (2007). Additional MXD data, originally produced by Schweingruber et al. (1987, 1991), were acquired for this study. These data represent the PH and Petkeljärvi (PJ) sites and have been used in several previously published large-scale/hemispheric tree-ring-based climate assessments (e.g. Briffa et al. 2002a, 2002b). These data were downloaded from an online data repository (Grissino-Mayer and Fritts 1997). The PH and PJ data contained multiple MXD records per tree. In this study, only one (the longest) record per tree was used to increase compatibility with other datasets. Both the new and previously published MXD data from the PH site were included in our analyses (Table S1).

Following the original papers where the corresponding microdensitometric laboratory facilities were originally described, the subsets are hereafter referred to as GUN (Gunnarson et al. 2011), PEL (Peltola et al. 2007), and SCH data (Schweingruber et al. 1987, 1991).

Dendrochronological analyses

Tree-ring series were detrended using the Regional Curve Standardization (RCS) methods (Briffa et al. 1992, 1996; Helama et al. 2017b). The cross-dated MXD data were re-aligned according to their ring number, counted from the pith. Pith offsets were taken into account when available. Biological growth trends, i.e. RCS curves, were modelled using the 'Hugershoff' function (Bräker 1981) fitted to a cloud of density observations, plotted as a function of ring number. The SCH, PEL, and GUN data were originally produced using slightly different protocols and machinery (Schweingruber et al. 1978; Peltola et al. 2007; Gunnarson et al. 2011). Following Gunnarson et al. (2011), the density values of these subsets (SCH, PEL, and GUN) were detrended using their own RCS curves (Fig. S1a–c).

Tree-ring indices were derived from the curves as residuals, aligned according to their calendar years, and averaged into mean chronologies representing the FO, PJ, PH, and SA sites (Fig. 1). The RCS produce was accompanied by signal-free implementation (Melvin and Briffa 2008; Melvin et al. 2013). Mean index values were subtracted from individual indices, both dated to calendar years. The resulting signal-free series were rescaled to the mean of the original density series, except for years in which the chronology sample count was one, where the original value was used. The signal-free values were again aligned according to their ring numbers, and the 'Hugershoff' function was fitted to these values (Fig. S1d–f). A new set of RCS indices was calculated as above. The process was repeated until the difference in the second decimal place of the mean indices between consecutive signal-free runs was less than one (Helama and Bartholin 2019).

In addition to mean MXD levels, their standard deviations may also vary depending on the analytical options chosen during the measurement process (Grudd 2008; Helama et al. 2010, 2012; Gunnarson et al. 2011). While the RCS curves used to detrend the GUN, PEL, and SCH series eliminated any possible differences between their mean levels, the standard deviations of the index records with at least thirty MXD values were compared over a period with a high sample number (AD 1895–1978). Before averaging the chronology, the scaling factors of 0.85, 1.11, and 1.28 were applied to the GUN, PEL, and SCH data, respectively. The mean correlation

between the index series was calculated for each calendar year and used to stabilise the variance of the tree-ring chronology, as previously suggested by Osborn et al. (1997).

Phenological observations

A plant phenological dataset, representing observations collated and originally published by the Finnish Society of Sciences and Letters (Elfving 1938; Elfving and Mickwitz 1988), was used as an another source of information representative of past temperature variations. This dataset was recently published in digital form (Holopainen et al. 2023a), with the modern nomenclature of taxonomy and standardised phenological terminology. The data contain information on 985 taxa and 16 different phenological stages from 371 locations across historical and modern Finland and adjacent areas. In this study, observations from the southern part of the country were used. In practice, the northernmost observations came from the site of Oulu, a town located at 65° N. A statistical outlier estimate was calculated by Holopainen et al. (2023a) for each observation date value as the z-score statistic, adopted from the methodology of Li et al. (2020) to evaluate the homogeneity of citizen science data. This statistic was applied here to exclude observations with scores above 3.0 or below –3.0 (i.e. $|z| > 3$). The remaining observations were included in the construction of our phenological record (i.e. mean time series).

First, Julian dates (prior to 1753) were converted to Gregorian dates. Second, the observation dates were converted to integers, expressed relative to the June solstice. This was to avoid slight biases that may arise, especially in long data series when Gregorian dates are used to form multicentennial time series (see Sagarin and Micheli 2001; Sagarin 2001, 2009). Third, the dates of phenological events (e.g. leaf outbreak of *Betula* sp.) were transformed into dimensionless data (z-scores). To do so, the dates were explained by the latitudes of their observation sites.

This modelling was performed using linear regression to account for the poleward decrease of temperatures and thus the latitudinal trends in the dates of the same phenological event across the country. Latitude was used here as this variable has previously been identified as the main determinant of both long-term mean temperatures (Laaksonen 1976) and phenological dates (Holopainen et al. 2018) across Finland. Residuals from the latitude-dependent trendline were calculated as the differences between the observed dates and those predicted by the model, and z-scores were produced by dividing each residual by the standard deviation of the residuals. This estimation was repeated separately for the dates of each phenological event, with at least 30 observations. Finally, a mean time series (1750–1955) was calculated from all phenological observations (n = 231 606) transformed into z-scores as described above.

Climatic correlations

Pearson correlations were first calculated between our new MXD site chronologies (FO, PH, and SA) and monthly mean temperatures. Site-specific climate records are available since 1960 from a spatial model constructed by the Finnish Meteorological Institute (Aalto et al. 2013, 2016). Accordingly, these correlations were calculated for the AD 1960–2021 period and did not include MXD data from our PJ site that was not updated. Longer instrumental records were obtained as regional (65–60° N, 20–30° E) mean temperatures available from the CRUTEM5 dataset since AD 1850 (Osborn et al. 2021) and from Berkeley data since AD 1750 (Rohde and Hausfather 2020). As the phenological data cover the AD 1750–1955 period, a second set of correlations was calculated for the AD 1850–1955 period, which was common to CRUTEM5, Berkeley, and proxy records represented by the regional mean/multi-site MXD chronology and phenological data. To minimise the impact of autocorrelation or trends on the assessment of *p*-values, the index series of proxy estimates were linearly detrended and pre-whitened (Monserud and Marshall 2001). These pre-whitened series were used only for the correlation analysis described above.

Calibration and verification of proxy data

Evaluation of the temporal stability of the relationship between the proxy and instrumental temperature records was carried out using a cross-calibration/verification procedure (Gordon et al. 1982; Briffa et al. 1988). Linear and multiple linear regression models were built to assess relationships between a dependent variable (mean temperature) and independent variables (regional mean RCS index and phenological z-score). Lagging ($t - 1$) and leading ($t + 1$) RCS index values were included in the models, together with the RCS index concurrent (t_0) with climate, since their inclusion can improve the models (for recent examples, see Zheng et al. 2015 and Karanitsch-Ackerl et al. 2019). Here, it was observed that the skill of lagging and leading RCS index values varied temporally (not shown); therefore, the mean of RCS index values from years $t - 1$ and $t + 1$ was used as an independent variable, together with the concurrent (t_0) RCS index.

Different combinations of proxy data were used to explain the variation in regional (65–60° N, 20–30° E) temperatures. In the first model, the RCS indices were used to explain the variation in CRUTEM5 (Osborn et al. 2021)-based temperatures; in the second model, the phenological z-score was used as an independent variable, while the third model incorporated both the phenological z-score and RCS index, explaining the variation in the instrumental data. Similar models were then built, with an exception that Berkeley (Rohde and Hausfather 2020)-based temperatures were used as the dependent variable.

The period common to all types of data was divided into early (AD 1850–1902) and late (AD 1903–1955) periods for the cross-calibration/verification exercise. The coefficient of determination (R^2) was calculated over the calibration period. Data withheld from calibration were used to calculate verification statistics (the squared correlation coefficient, r^2; reduction of error, RE; coefficient of efficiency, CE) (Fritts 1976; Briffa et al. 1988). The significance of these statistics was assessed using Monte Carlo implementation (Efron and Tibshirani 1986). Following the approach of Ebisuzaki (1997), 10 000 pairs of surrogate time series (i.e. 20 000 series) with

the same power spectrum as the original time series but with a random phase were generated to produce empirical probability distribution (single-tailed) for each statistic and to obtain the significance.

Finally, the proxy records were used in the models built over an extended period (AD 1850–2020), and the three proxy-based reconstructions were compared. Since the RCS chronology overlaps a longer period (AD 1850–2020) with instrumental temperature data, the MXD data were additionally divided into early (AD 1850–1935) and late (AD 1936–2020) periods for calibration and verification tests. Moreover, the long period (AD 1850–2020) was used as the final calibration period for the long MXD-based temperature reconstruction. For each reconstruction, Monte Carlo-based confidence intervals were calculated at the 95% and 99% thresholds from the autoregressive structure of the residuals of each transfer function. All Monte Carlo implementations were run using the algorithm of Macias-Fauria et al. (2012).

Additional verification of the new palaeoclimate data was carried out using the longest available records of the Berkeley temperature dataset (Rohde and Hausfather 2020), extending back to AD 1750, as well as instrumental data from the Finnish historical observation site of Turku (AD 1749–1794, AD 1797–1823) (Holopainen 2004, 2006) and the northwestern Russian site of St Petersburg (Jones and Lister 2002). Running Pearson correlations, calculated with a 30-year window length, were used to evaluate the strength of associations and their possible temporal variations between the proxy and instrumental data.

MXD data from other sites

Wilson et al. (2016) previously collected late Holocene tree-ring records from temperature-sensitive northern hemispheric sites. Similar to our study, this dataset is predominantly composed of MXD-based records, with a limited number of data produced using other tree-ring parameters sensitive to warm-season temperatures. Data representing Fennoscandian and adjacent sites (Kola Peninsula) were adopted here, with the exception of two datasets analysed separately: Esper et al. (2012) (referred to as NSCAN region in northern Finland and Sweden) and Melvin et al. (2013) (Torneträsk (TORN) region in northernmost Sweden). Since their original publication, these two northern Fennoscandian MXD datasets have been occasionally utilised as an integrated record (Esper et al. 2014; Matskovsky and Helama 2014; Wilson et al. 2016). Our purpose to analyse them separately was to provide a more detailed view on their relatedness to our data.

Other records included in our comparison originate from Forfjorddalen (FORF) in northern Norway (McCarroll et al. 2013), the Khibiny Mountains in Kola Peninsula (KOL) (McCarroll et al. 2013), Tjeggelvas/Arjeplog/Ammarnäs (TAA) sites in northern Sweden (Linderholm et al. 2014), and the province of Jämtland (JAEM) in central Scandinavia (Zhang et al. 2016). A spline function (Cook and Peters 1981) with 50-year rigidity was applied to smooth the records to illustrate and analyse their long-term (i.e. low-frequency) variability.

Pearson correlations between the records were calculated with associated *p*-values, using the Monte Carlo implementation of Macias-Fauria et al. (2012) with the reproduction of 10 000 pairs of surrogate time series. To present Fennoscandian temperature curves, the arithmetic mean and first principal component (PC#1) of the records spanning AD 820–2005 were calculated. For illustrative purposes, all records were normalised to a zero mean and unit variance over the AD 1200–2005 period.

Results

Climatic correlations

Warm-season temperatures (1960–2021) correlated positively with the MXD data, as demonstrated for each updated site (Fig. 2a). The strongest relationships were observed between mid- to late-summer temperatures, which were more strongly positive than those for spring and early-summer conditions. July emerged as the month with statistically significant correlations ($p < 0.01$) across all the MXD chronologies. The finding that wood production at the FO site, which has not previously been included in palaeoclimatic reconstructions, can be associated with summer temperature variability suggests the potential of using this proxy for temperature reconstructions, akin to previously published palaeotemperature results from other sites in the study region (Helama et al. 2014b).

Relationships between the MXD data and warm-season temperatures were notably high, as shown by the mean regional/multi-site chronology for the AD 1850–1955 period (Fig. 2b). Comparing the results for MXD and phenological

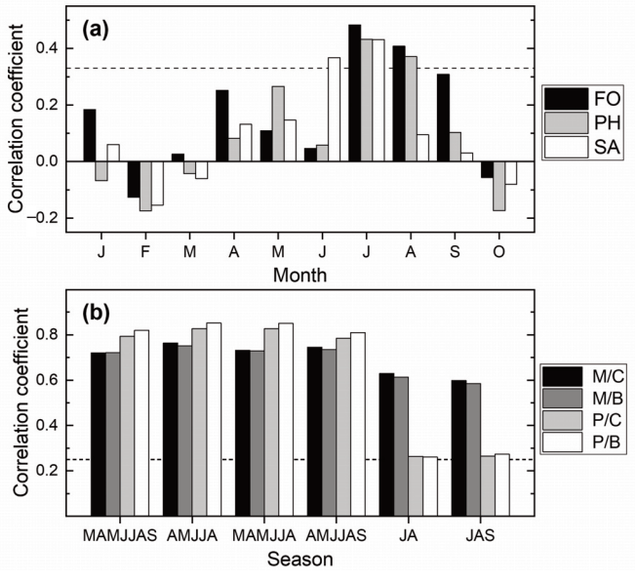

Fig. 2. **(a)** Pearson correlations of our new latewood maximum density data from the FO, PH, and SA sites (see Fig. 1 for locations), with monthly mean temperatures estimated for each site over the AD 1960–2021 period, excluding the PJ site that was not updated. **(b)** Pearson correlations of latewood maximum density (M) and phenological (P) records with regional (65–60° N, 20–30° E) seasonal mean temperatures for March–September (MAMJJAS), April–August (AMJJA), March–August (MAMJJA), April–September (AMJJAS), July–August (JA), and July–September (JAS) obtained from CRUTEM5 (C) and Berkeley (B) datasets over the AD 1850–1955 period. The level of statistical significance ($p < 0.01$) is marked with a horizontal dashed line.

data showed that temperature correlations for MXD data were ~0.7, while those for phenological data were slightly higher, averaging ~0.8. Considerably lower correlations were found when the proxy data were compared only with mid- to late-season temperatures, especially for phenological data. The use of either the CRUTEM5 or Berkeley datasets did not result in remarkable differences; the former correlated slightly better with MXD and the latter with phenological data, but the differences appeared marginal.

Considering the potential for palaeotemperature reconstructions, these relationships suggest that robust temperature estimates are most likely obtained when instrumental temperature data representing months from early to late warm season are included in statistical models. In this regard, the March–August and April–August mean temperatures, showing the highest overall correlations, were chosen for the calibration/verification tests.

Proxy/climate models

On average, 68% of the April–August temperature variance was explained over the AD 1850–1955 period (see Fig. 3). This figure was slightly higher than that for March–August temperatures, which averaged 65%. Both the R^2 and r^2 statistics were statistically highly significant ($p < 0.0001$) (Tables S2–S5). Phenological data outperformed MXD in their reconstruction skill, with their respective models explaining 69% and 55% of temperature variance over the same period. The multi-proxy models showed R^2 and r^2 averaging 0.75, which outperformed the single-proxy models, which had R^2 and r^2 averaging 0.62. The models were slightly improved when temperatures from the Berkeley dataset were used as the dependent variable, in comparison to the CRUTEM5 dataset. The former explained 68% and the latter 65% of the warm-season temperature variance.

The positive and statistically highly significant (at least at the 0.0002 level) RE and CE statistics obtained for different combinations of dependent and independent variables over both subperiods indicated acceptable reconstruction skill. On average, models built over the full calibration period (AD 1850–1955) explained 69% of the temperature variance (Fig. 4). Again, models using MXD data showed an R^2 of ~0.6, lower than that for phenological data (R^2 ~0.7), whereas the multi-proxy model had an R^2 of ~0.8, clearly exceeding the single-proxy models.

Results for MXD data over an extended period (AD 1850–2020) showed a slightly different pattern. Both R^2 and r^2 were, on average, higher when reconstructing April–August temperatures (Fig. 3; Tables S2–S5). In any case, the use of March–August temperatures resulted in unsatisfactory verification statistics, especially over the early verification period (AD 1850–1935), but only when using CRUTEM5 temperatures (Table S2). Models exploiting Berkeley data explained 63% of the temperature variance over the full period, in comparison to 59% for the CRUTEM5 temperature data (Fig. 4). Based on these results, April–August (Berkeley) temperatures (Fig. 5) were reconstructed for southern Finland (Table S6). All reconstructions showed markedly high temperature correlations across an extended region of northern Europe (Fig. S2a–c). As an expected outcome, the correlations were slightly higher, and their spatial extent slightly wider, for reconstructions based on phenological and multi-proxy data.

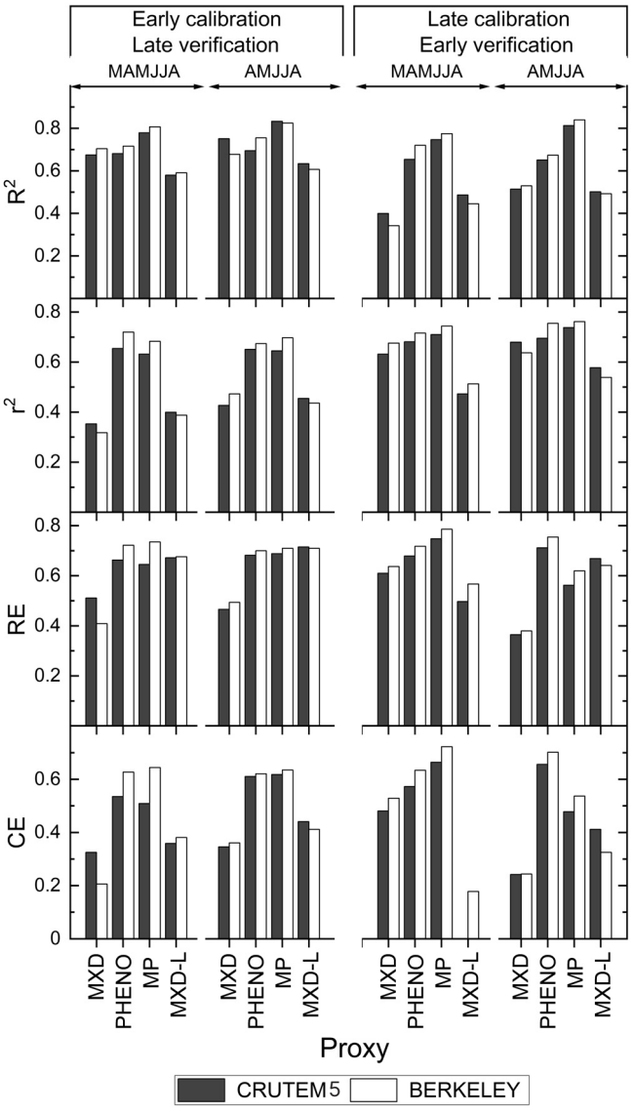

Fig. 3. Calibration and verification statistics for March–August (MAMJJA) and April–August (AMJJA) temperature reconstructions. Instrumental temperatures, obtained from the CRUTEM5 and Berkeley datasets, are explained over the early (AD 1850–1902) and late (AD 1903–1955) periods by the RCS indices of maximum latewood density (MXD), phenological z-scores (PHENO), and multiple proxy (MP) data using both RCS indices, and over the early (AD 1850–1935) and late (AD 1936–2020) periods by the RCS indices (MXD-L). The full calibration period is divided into two subperiods for cross-validation. The coefficient of determination (R^2) is calculated over the calibration period, while the squared coefficient of correlation (r^2), the reduction of error (RE), and the coefficient of efficiency (CE) statistics are calculated over the verification period. See Tables S2–S5 for details and *p*-values.

Comparison with long instrumental records

Correlations between the reconstructions and long instrumental temperature (Berkeley) records remained ~0.7 or

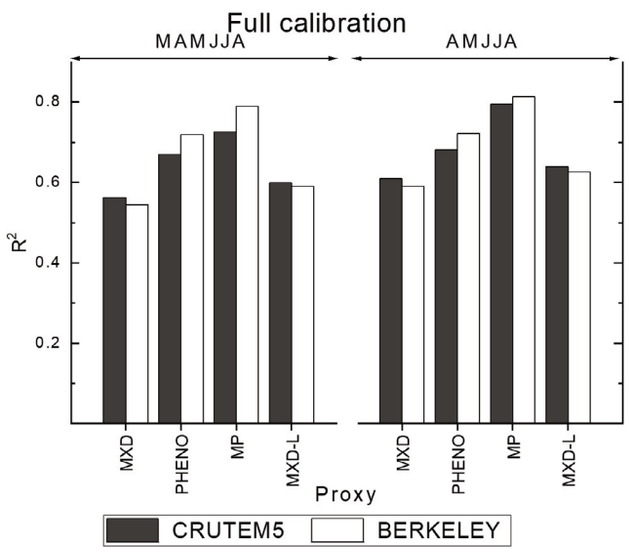

Fig. 4. Statistics over the full calibration period using the coefficient of determination (R^2). March–August (MAMJJA) and April–August (AMJJA) temperatures, obtained from the CRUTEM5 and Berkeley datasets, are explained over the AD 1850–1955 period by the RCS indices of maximum latewood density (MXD), phenological z-scores (PHENO), and multiple proxy (MP) data using both RCS indices, and over the AD 1850–2020 period by the RCS indices (MXD-L). All results were statistically significant ($p < 0.0001$) based on Monte Carlo simulations.

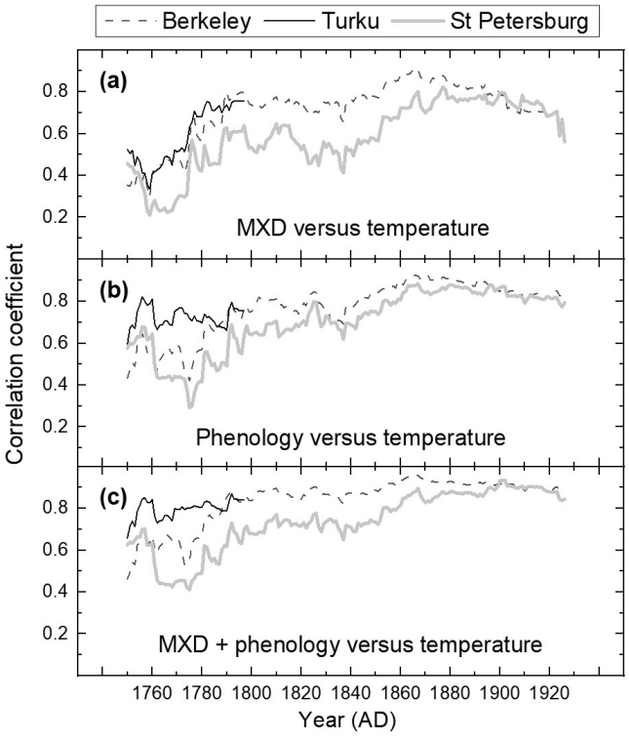

Fig. 6. Running 30-year correlations between the reconstructed and instrumental April–August temperatures. Reconstructions were based on **(a)** latewood maximum density (MXD), **(b)** phenological index, and **(c)** multiple proxy (MXD + phenology) data, covering the AD 1750–1955 period. Instrumental data represent regional temperatures from the Berkeley dataset (65–60° N, 20–30° E) and from temperature observations made in Turku (southwestern Finland) and St Petersburg (northwestern Russia).

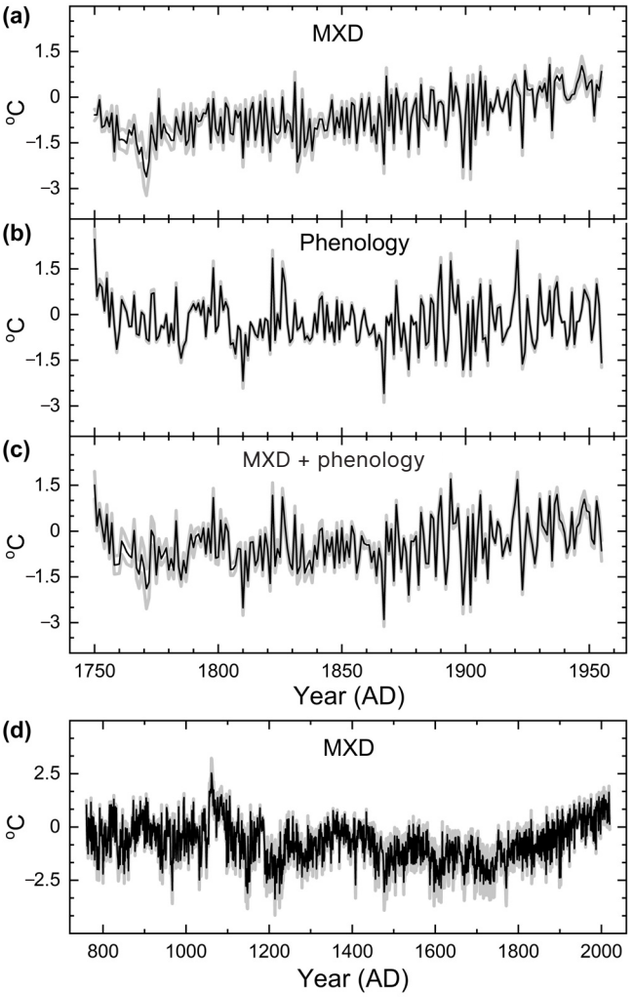

Fig. 5. April–August temperature reconstructions of Berkeley temperature data (Rohde and Hausfather 2020) based on **(a)** latewood maximum density (MXD), **(b)** phenological index, and **(c)** multiple proxy (MXD + phenology) data over the AD 1750–1955 period, and **(d)** MXD-based reconstruction since AD 760, shown with their 95% (grey boundaries) confidence intervals. See Table S6 for annual temperature estimates.

higher since AD 1790 (Fig. 6). However, prior to that date, correlations with both Berkeley and St Petersburg temperatures were markedly lower. Interestingly, a similar 18th-century decline in temperature associations was not observed when the reconstructions based on phenological or multi-proxy data were compared with Turku temperatures.

Late Holocene temperature reconstructions

Based on our long MXD-based temperature history (Fig. 5d), the warmest and coldest 100-year periods were evident for AD 1920–2019 and AD 1650–1749, respectively, with their mean temperatures differing by 2.1 °C. The coldest 30-year period occurred between AD 1715 and 1744. Since then, warm-season temperatures have increased by 2.8 °C until the present day (1991–2020).

Comparing our new reconstruction with data from around the region of Fennoscandia and Kola Peninsula showed statistically significant correlations (Fig. 7). On average, correlations between the new reconstruction and other records

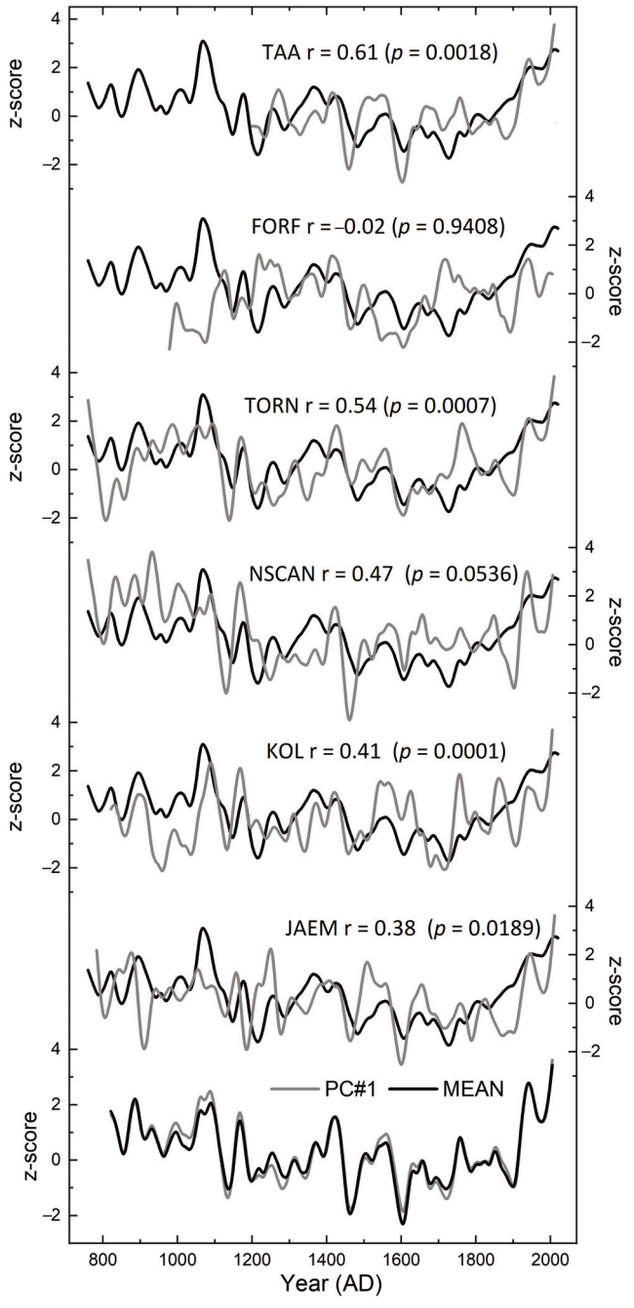

Fig. 7. Low-frequency comparison between our new MXD-based palaeotemperature curve (black line) and other similarly produced records (grey line) from Fennoscandia and Kola Peninsula. Abbreviations: TAA – Tjeggelvas/Arjeplog/Ammarnäs sites in northern Sweden (AD 1200–2010), FORF – Forfjorddalen in northern Norway (AD 978–2005), TORN – Torneträsk region in northernmost Sweden (here, AD 760–2010), NSCAN – collection of sites in northern Scandinavia (here, AD 760–2006), KOL – Khibiny Mountains in Kola Peninsula (AD 820–2005), JAEM – Jämtland in central Scandinavia (AD 783–2011), PC#1 – first principal component of the records spanning AD 820–2005, MEAN – arithmetic mean of the records (AD 820–2005). Statistical comparisons were carried out using Pearson correlations (r) with associated *p*-values.

averaged 0.40. The highest correlations were found with TAA and TORN data representing sites in northern Sweden. Intriguingly, NSCAN data that originate mainly from northern Finland did not show similarly high relatedness despite the closer proximity. A promising association was also evident with JAEM data from central Scandinavia, representing similar latitudes but higher altitudes in mountainous terrain. The lowest correlation was found with FORF data that represent conditions in northern Norway, potentially due to excessive maritime influence on local climate.

Correlations among these data (excluding our reconstruction) averaged 0.35, which is slightly lower than the correlation between our record and other Fennoscandian records (0.40), suggesting that the new reconstruction contains a regionally representative long-term climatic signal comparable to other palaeotemperature estimates from the same region. Finally, the PC#1 and MEAN curves representing Fennoscandian temperature fluctuations (including our new MXD-based reconstruction) were very similar. These curves illustrated relatively warm temperatures from the 9th to the 11th centuries AD that predated a cool climatic phase lasting until the beginning of the 20th century AD, followed by a profound warming towards the present. The PC#1 record showed high correlations with instrumental temperatures over Fennoscandia and the Norwegian Sea but was less representative over central-eastern Europe compared to our reconstructions from southern Finnish sites (Fig. S2d).

Discussion

Plant-based data from southern Finland explained April–August temperatures to an extent that allowed their use in quantitative palaeoclimate reconstructions. These records originate from low-lying sites and represent south and middle boreal zones distant from polar or alpine ecotones, where plant activity is expected to more closely reflect growing season temperatures. Judged by R^2 ~0.6, our MXD data appeared to correspond markedly well with summer temperatures, this figure being comparable to the R^2 range of 50–66% obtained previously for similar data from higher latitudes/altitudes in Fennoscandia and Kola Peninsula (see Wilson et al. 2016, table 1). The multi-site approach used to build the MXD dataset may have averaged out non-climatic noise related to site histories, thus increasing the proxy/climate correlations. Nonetheless, the responsiveness of plant phenology to temperature (R^2 ~0.7) was even greater than that of wood production, demonstrating the value of these proxy data for palaeoclimate studies.

Similar to MXD, phenological observations have occasionally been used as proxy data for temperature reconstructions. By necessity, such studies have focused on sites and regions where historical records of plant phenological observations are available (Tarand and Kuiv 1994; Tarand and Nordli 2001; Chuine et al. 2004; Aono and Kazui 2008; Zheng et al. 2015; Aono and Nishitani 2022). These sites are often quite distant from the high-latitude and high-altitude sites where temperature-sensitive tree-ring samples are typically collected, which creates a disparity that complicates the integration of these two high-resolution proxy records. In fact, our previous attempt to combine phenological and tree-ring records in southern Finland was doomed from the start, as the ring-width data we had did not show time-invariant correlations with any warm-season temperature variable (Holopainen

et al. 2006). These limitations were now overcome with the use of MXD data. Moreover, the resulting multi-proxy models outperformed (R^2 ~0.8) the models based on either variable alone. Our approach is similar to that of Zheng et al. (2015), who reconstructed annual temperature variations using both tree-ring and phenological data in south-central China since AD 1850.

Phenological data are typically restricted to populated areas, but these data are also subject to limitations pertaining to the eagerness of historical actors to record observations. The availability of historical observations may have been influenced by opportunistic variations and varying levels of support from citizen scientists (Holopainen et al. 2023b). In Finland, the systematic collection of phenological observations started following Carl von Linné's suggestions to establish a station network for this purpose. Since 1750, citizen science activity has been maintained by several Finnish societies and universities (Holopainen et al. 2012, 2018). While this activity has resulted in an enormous collection of phenological data, the history of such observations sets a temporal limit on the length of the record. At present, we are not aware of any plant phenological observations to have been made in Finland prior to AD 1750. In Estonia, Tarand and Kuiv (1994) reported phenological observations of agricultural events dating back to AD 1671, which suggests that the Finnish plant phenological dataset could, in theory, be extended further.

Although the number of phenological observations was markedly low prior to AD 1877 (Fig. 1c), their correlations – especially with local temperatures from Turku (Holopainen 2004, 2006) – were not remarkably reduced (Fig. 6b). However, correlations did drop when compared against Berkeley temperature estimates. This divergence likely suggests that the temperatures obtained from a global database may not optimally represent our proxy sites and data. In fact, a relatively high proportion of phenological observations sites are located in the southwestern part of the study region (see Fig. 1a), near Turku. The geographical overlap between the proxy and instrumental sites may have stabilised the correlations between the respective records over the period in question, during which Berkeley data (Rohde and Hausfather 2020) are predominantly based on estimates from Russian (St Petersburg) and Swedish (Uppsala and Stockholm) sites. Therefore, it seems that the lack of local temperature data in the Berkeley database may well be the most likely factor in the observed decrease in correlations.

While we do not intend to question the merits of the global temperature database (Rohde and Hausfather 2020), especially since verification outputs were statistically significant over the AD 1850–1935 period only using these data (Fig. 3), the results also demonstrate the value of local climate records for proxy/climate assessments when temperature estimates are interpolated from a sparser network of observations. It seems that such conditions existed in our case during the 18th century AD. Regrettably, early instrumental records may be discontinuous; for instance, in our historical site, observation activity ceased after the Great Fire of Turku in 1827 (Holopainen 2004). The importance of proxy records during these critical periods is multifaceted, as proxy-based reconstructions provide continuous time series for comparisons across the full length of the instrumental period and beyond.

Our MXD-based estimates demonstrated an ongoing warming trend since the 18th and 19th centuries AD, placing this event in a long-term perspective. Instrumental data have shown that warming observed in Finland since the mid-19th century AD has been stronger in late autumn and spring than in the summer months (Mikkonen et al. 2015). In addition, other studies have indicated statistically significant warming trends in Finnish summer temperatures over various intervals of the instrumental era (Tietäväinen et al. 2010; Irannezhad et al. 2015). According to Tuomenvirta (2004), the only seasonal long-term (150-year) trend in Finnish temperatures was found for the spring season. Defined by rigorous calibration/verification examination, our reconstruction season (April–August) encompasses both spring and summer months.

Although our study region does not cover the northern half of the country, the agreement between the instrumental and proxy-based trends is obvious. Calculated from values provided by Mikkonen et al. (2015), the change in April–August temperatures between their early (AD 1847–1856) and late (AD 2004–2013) periods averaged 1.6 ± 0.5 °C. Our reconstructed values (Fig. 5d) demonstrate a corresponding change of 1.9 ± 0.4 °C, which falls within the 95% confidence interval of the instrumentally observed change. The coldest 100-year period in our reconstruction occurred between AD 1650 and 1749, with low temperatures prevailing throughout much of the 17th and 18th centuries AD (see Fig. 5d). This period overlaps with the Little Ice Age (LIA) (Bradley and Jones 1993; Grove 2004), corresponding to the AD 1570–1900 period, during which Northern Hemisphere summer temperatures remained significantly below the AD 1961–1990 mean (Matthews and Briffa 2005), and even more closely to the Maunder Minimum, a prolonged period of sunspot minimum between AD 1645 and 1715 (Eddy 1976), suggesting that solar forcing (Gray et al. 2010) may have contributed to the low warm-season temperatures during this period.

Even a longer period of cooling since the 12th century AD was evident in the PC#1 and MEAN curves representing Fennoscandian temperature fluctuations from the end of the first millennium AD (Fig. 7). This phase aligns with palaeoclimatic evidence suggesting that cooling towards the LIA may have begun as early as ~AD 1300 (Matthews and Briffa 2005). The long-term LIA cooling was predated by relatively warmer temperatures from the 9th to the 11th centuries AD, overlapping with the evidence for the Medieval Climate Anomaly, during which conditions as warm as those of the past decades may have prevailed in some regions of the globe around AD 950–1250 (Mann et al. 2009). While similar tree-ring evidence for the Medieval Climate Anomaly and LIA has been documented from northern Fennoscandia since the pioneering achievements of Briffa et al. (1992) and later by several other authors, we also highlight that both the PC#1

and MEAN curves indicate warm climates during the first halves of the 15th and 16th centuries AD, interrupting the long-term LIA cooling. The relative warmth of these periods resonates with descriptions of a two-stage LIA (McDermott et al. 2001). Thus, our findings reinforce the previously presented evidence for a two-stage LIA in the study region and adjacent areas (Helama 2017; Helama et al. 2020), and more generally the millennial temperature evolution, including the Medieval Climate Anomaly, two-stage LIA, and recurring warming over the past century (Helama et al. 2009). These temperature changes reflect past fluctuations in North Atlantic forcing, reinforcing the view that the natural instability of thermohaline circulation (Bianchi and McCave 1999) has influenced long-term temperature evolution in Fennoscandia.

Finally, we note that the early centuries of our MXD chronology are represented by a reduced sample number (Fig. 1b). The diminished availability of subfossils may have been caused by simultaneous dry conditions, which could have lowered water levels, thus reducing the preservation potential of subfossil trees in lake environments (Helama et al. 2017a). In contrast, dry surface conditions are beneficial for peatland pine colonisation, increasing the supply of subfossil trees (Edvardsson et al. 2016). Interestingly, the results gathered so far from southeastern Finland indicate that an increasing number of subfossil pine trees from peatland sites are dated to ~1000 years before present (Helama et al. 2017a). Therefore, to increase the number of tree-ring samples indicative of climate conditions in southern Finland during the late first and early second millennia AD, there seems to be a need to shift the focus from lake to peatland archives of *Pinus sylvestris* subfossils.

Data availability statement

The data for the temperature reconstructions are available in Supplementary items, Table S6.

Acknowledgements

Public and private landowners are thanked for granting permissions for tree-ring coring. We are also grateful for the comments provided by Anneli Poska and an anonymous reviewer. This study was supported by the Academy of Finland (grant No. #339788). The publication costs of this article were partially covered by the Estonian Academy of Sciences.

Supplementary online data

Supplementary online data to this article can be found at https://doi.org/10.3176/earth.2025.06S

References

Aalto, J., Pirinen, P., Heikkinen, J. and Venäläinen, A. 2013. Spatial interpolation of monthly climate data for Finland: comparing the performance of kriging and generalized additive models. *Theoretical and Applied Climatology*, **112**, 99–111. https://doi.org/10.1007/s00704-012-0716-9

Aalto, J., Pirinen, P. and Jylhä, K. 2016. New gridded daily climatology of Finland: permutation-based uncertainty estimates and temporal trends in climate. *Journal of Geophysical Research: Atmospheres*, **121**(8), 3807–3823. https://doi.org/10.1002/2015jd024651

Ahti, T., Hämet-Ahti, L. and Jalas, J. 1968. Vegetation zones and their sections in northwestern Europe. *Annales Botanici Fennici*, **5**(3), 169–211.

Anchukaitis, K. J., Wilson, R., Briffa, K. R., Büntgen, U., Cook, E. R., D'Arrigo, R. et al. 2017. Last millennium Northern Hemisphere summer temperatures from tree rings: part II, spatially resolved reconstructions. *Quaternary Science Reviews*, **163**, 1–22. https://doi.org/10.1016/j.quascirev.2017.02.020

Aono, Y. and Kazui, K. 2008. Phenological data series of cherry tree flowering in Kyoto, Japan, and its application to reconstruction of springtime temperatures since the 9th century. *International Journal of Climatology*, **28**(7), 905–914. https://doi.org/10.1002/joc.1594

Aono, Y. and Nishitani, A. 2022. Reconstruction of April temperatures in Kyoto, Japan, since the fifteenth century using the floral phenology of herbaceous peony and rabbit-ear iris. *International Journal of Biometeorology*, **66**, 883–893. https://doi.org/10.1007/s00484-022-02245-x

Babst, F., Poulter, B., Trouet, V., Tan, K., Neuwirth, B., Wilson, R. et al. 2013. Site- and species-specific responses of forest growth to climate across the European continent. *Global Ecology and Biogeography*, **22**(6), 706–717. https://doi.org/10.1111/geb.12023

Bianchi, G. G. and McCave, I. N. 1999. Holocene periodicity in North Atlantic climate and deep-ocean flow south of Iceland. *Nature*, **397**, 515–517. https://doi.org/10.1038/17362

Bradley, R. S. and Jones, P. D. 1993. 'Little Ice Age' summer temperature variations: their nature and relevance to recent global warming trends. *The Holocene*, **3**(4), 367–376. https://doi.org/10.1177/095968369300300409

Bräker, O. U. 1981. Der Alterstrend bei Jahrringdichten und Jahrringbreiten von Nadelhölzern und sein Ausgleich. *Mitteilungen der forstlichen Bundesversuchsanstalt Wien*, **142**, 75–102.

Briffa, K. R., Jones, P. D., Pilcher, J. R. and Hughes, M. K. 1988. Reconstructing summer temperatures in northern Fennoscandinavia back to A.D. 1700 using tree-ring data from Scots pine. *Arctic and Alpine Research*, **20**(4), 385–394. https://doi.org/10.1080/00040851.1988.12002691

Briffa, K. R., Jones, P. D., Bartholin, T. S., Eckstein, D., Schweingruber, F. H., Karlén, W. et al. 1992. Fennoscandian summers from AD 500: temperature changes on short and long timescales. *Climate Dynamics*, **7**, 111–119. https://doi.org/10.1007/BF00211153

Briffa, K. R., Jones, P. D., Schweingruber, F. H., Karlén, W. and Shiyatov, S. G. 1996. Tree-ring variables as proxy-climate indicators: problems with low-frequency signals. In *Climate Variations and Forcings Mechanisms of the Last 2000 Years* (Jones, P. D., Bradley, R. S. and Jouzel, J., eds). Springer, Berlin, 9–41.

Briffa, K. R., Osborn, T. J., Schweingruber, F. H., Jones, P. D., Shiyatov, S. G. and Vaganov, E. A. 2002a. Tree-ring width and density data around the Northern Hemisphere: part 1, local and regional climate signals. *The Holocene*, **12**(6), 737–751. https://doi.org/10.1191/0959683602hl587rp

Briffa, K. R., Osborn, T. J., Schweingruber, F. H., Jones, P. D., Shiyatov, S. G. and Vaganov, E. A. 2002b. Tree-ring width and density data around the Northern Hemisphere: part 2, spatio-temporal variability and associated climate patterns. *The Holocene*, **12**(6), 759–789. https://doi.org/10.1191/0959683602hl588rp

Chuine, I., Yiou, P., Viovy, N., Seguin, B., Daux, V. and Le Roy Ladurie, E. 2004. Historical phenology: grape ripening as a past climate indicator. *Nature*, **432**, 289–290. https://doi.org/10.1038/432289a

Cook, E. R. and Peters, K. 1981. The smoothing spline: a new approach to standardizing forest interior tree-ring width series for dendroclimatic studies. *Tree-Ring Bulletin*, **41**, 45–53.

Ebisuzaki, W. 1997. A method to estimate the statistical significance of a correlation when the data are serially correlated. *Journal of Climate*, **10**(9), 2147–2153. https://doi.org/10.1175/1520-0442(1997)010<2147:AMTETS>2.0.CO;2

Eddy, J. A. 1976. The Maunder Minimum. *Science*, **192**(4245), 1189–1202. https://doi.org/10.1126/science.192.4245.1189

Edvardsson, J., Stoffel, M., Corona, C., Bragazza, L., Leuschner, H. H., Charman, D. J. and Helama, S. 2016. Subfossil peatland trees as proxies for Holocene palaeohydrology and palaeoclimate. *Earth-Science Reviews*, **163**, 118–140. https://doi.org/10.1016/j.earscirev.2016.10.005

Efron, B. and Tibshirani, R. 1986. Bootstrap methods for standard errors, confidence intervals, and other measures of statistical accuracy. *Statistical Science*, **1**(1), 54–75. https://doi.org/10.1214/ss/1177013815

Elfving, F. 1938. Fenologiset havainnot. *Societas Scientiarum Fennica, Commentationes Humanarum Litterarum*, **10**, 204–213.

Elfving, G. and Mickwitz, G. 1988. *Suomen Tiedeseuran kolmas puolivuosisata 1938–1987*. Suomen Tiedeseura, Ekenäs.

Esper, J., Frank, D. C., Timonen, M., Zorita, E., Wilson, R. J. S., Luterbacher, J. et al. 2012. Orbital forcing of tree-ring data. *Nature Climate Change*, **2**, 862–866. https://doi.org/10.1038/nclimate1589

Esper, J., Düthorn, E., Krusic, P. J., Timonen, M. and Büntgen, U. 2014. Northern European summer temperature variations over the Common Era from integrated tree-ring density records. *Journal of Quaternary Science*, **29**(5), 487–494. https://doi.org/10.1002/jqs.2726

Fritts, H. C. 1976. *Tree rings and climate*. Academic Press, New York.

Gordon, G. A., Gray, B. M. and Pilcher, J. R. 1982. Verification of dendroclimatic reconstructions. In *Climate from Tree Rings* (Hughes, M. K., Kelly, P. M., Pilcher, J. R. and LaMarche, V. V., Jr., eds). Cambridge University Press, Cambridge, 115–132.

Gray, L. J., Beer, J., Geller, M., Haigh, J. D., Lockwood, M., Matthes, K. et al. 2010. Solar influences on climate. *Reviews of Geophysics*, **48**(4), RG4001. https://doi.org/10.1029/2009RG000282

Grissino-Mayer, H. D. and Fritts, H. C. 1997. The International Tree-Ring Data Bank: an enhanced global database serving the global scientific community. *The Holocene*, **7**(2), 235–238. https://doi.org/10.1177/095968369700700212

Grove, J. M. 2004. *Little Ice Ages: Ancient and Modern*. Routledge, London.

Grudd, H. 2008. Torneträsk tree-ring width and density AD 500–2004: a test of climatic sensitivity and a new 1500-year reconstruction of north Fennoscandian summers. *Climate Dynamics*, **31**, 843–857. https://doi.org/10.1007/s00382-007-0358-2

Guay, R., Gagnon, R. and Morin, H. 1992. A new automatic and interactive tree ring measurement system based on a line scan camera. *The Forestry Chronicle*, **68**(1), 138–141. https://doi.org/10.5558/tfc68138-1

Gunnarson, B. E., Linderholm, H. W. and Moberg, A. 2011. Improving a tree-ring reconstruction from west-central Scandinavia: 900 years of warm-season temperatures. *Climate Dynamics*, **36**, 97–108. https://doi.org/10.1007/s00382-010-0783-5

Helama, S. 2017. An overview of climate variability in Finland during the Common Era. *Geophysica*, **52**(1), 3–20.

Helama, S. 2023. Distinguishing Type I and II errors in statistical tree-ring dating. *Quaternary Geochronology*, **78**, 101470. https://doi.org/10.1016/j.quageo.2023.101470

Helama, S. and Bartholin, T. S. 2019. Åland churches as archives of tree-ring records sensitive to fluctuating climate. *Acta Palaeobotanica*, **59**(1), 131–143. https://doi.org/10.2478/acpa-2019-0002

Helama, S., Lindholm, M., Meriläinen, J., Timonen, M. and Eronen, M. 2005. Multicentennial ring-width chronologies of Scots pine along north-south gradient across Finland. *Tree-Ring Research*, **61**(1), 21–32. https://doi.org/10.3959/1536-1098-61.1.21

Helama, S., Vartiainen, M., Kolström, T., Peltola, H. and Meriläinen, J. 2008. X-ray microdensitometry applied to subfossil tree-rings: growth characteristics of ancient pines from the southern boreal forest zone in Finland at intra-annual to centennial time-scales. *Vegetation History and Archaeobotany*, **17**, 675–686. https://doi.org/10.1007/s00334-008-0147-9

Helama, S., Timonen, M., Holopainen, J., Ogurtsov, M. G., Mielikäinen, K., Eronen, M. et al. 2009. Summer temperature variations in Lapland during the Medieval Warm Period and the Little Ice Age relative to natural instability of thermohaline circulation on multi-decadal and multi-centennial scales. *Journal of Quaternary Science*, **24**(5), 450–456. https://doi.org/10.1002/jqs.1291

Helama, S., Vartiainen, M., Kolström, T. and Meriläinen, J. 2010. Dendrochronological investigation of wood extractives. *Wood Science and Technology*, **44**, 335–351. https://doi.org/10.1007/s00226-009-0293-y

Helama, S., Bégin, Y., Vartiainen, M., Peltola, H., Kolström, T. and Meriläinen, J. 2012. Quantifications of dendrochronological information from contrasting microdensitometric measuring circumstances of experimental wood samples. *Applied Radiation and Isotopes*, **70**(6), 1014–1023. https://doi.org/10.1016/j.apradiso.2012.03.025

Helama, S., Holopainen, J., Timonen, M. and Mielikäinen, K. 2014a. An 854-year tree-ring chronology of Scots pine for south-west Finland. *Studia Quaternaria*, **31**(1), 61–68. https://doi.org/10.2478/squa-2014-0006

Helama, S., Vartiainen, M., Holopainen, J., Mäkelä, H., Kolström, T. and Meriläinen, J. 2014b. A palaeotemperature record for the Finnish Lakeland based on microdensitometric variations in tree rings. *Geochronometria*, **41**(3), 265–277. https://doi.org/10.2478/s13386-013-0163-0

Helama, S., Luoto, T. P., Nevalainen, L. and Edvardsson, J. 2017a. Rereading a tree-ring database to illustrate depositional histories of subfossil trees. *Palaeontologia Electronica*, **20**(1), 2A. https://doi.org/10.26879/696

Helama, S., Melvin, T. M. and Briffa, K. R. 2017b. Regional curve standardization: state of the art. *The Holocene*, **27**(1), 172–177. https://doi.org/10.1177/0959683616652709

Helama, S., Kuoppamaa, M. and Sutinen, R. 2020. Subaerially preserved remains of pine stemwood as indicators of late Holocene timberline fluctuations in Fennoscandia, with comparisons of tree-ring and ^{14}C dated depositional histories of subfossil trees from dry and wet sites. *Review of Palaeobotany and Palynology*, **278**, 104223. https://doi.org/10.1016/j.revpalbo.2020.104223

Helama, S., Ratilainen, R., Ruohonen, J. and Taavitsainen, J.-P. 2024. Developing millennial tree-ring chronology for Turku (Åbo) and comparing palaeoclimatic signals inferred from archaeological, subfossil and living *Pinus sylvestris* data in Southwest Finland. *Studia Quaternaria*, **41**(1), 1–11. https://doi.org/10.24425/sq.2024.149969

Holmes, R. L. 1983. Computer-assisted quality control in tree-ring dating and measurement. *Tree-Ring Bulletin*, **43**, 69–78.

Holopainen, J. 2004. *The Early Climatological Records of Turku*. Edita, Helsinki.

Holopainen, J. 2006. *Reconstructions of past climates from documentary and natural sources in Finland since the 18th century*. PhD thesis. University of Helsinki, Finland.

Holopainen, J., Helama, S. and Timonen, M. 2006. Plant phenological data and tree-rings as palaeoclimate indicators since AD 1750 in SW Finland. *International Journal of Biometeorology*, **51**, 61–72. https://doi.org/10.1007/s00484-006-0037-8

Holopainen, J., Helama, S., Kajander, J. M., Korhonen, J., Launiainen, J., Nevanlinna, H. et al. 2009. A multiproxy reconstruction of spring temperatures in south-west Finland since 1750. *Climatic Change*, **92**, 213–233. https://doi.org/10.1007/s10584-008-9477-y

Holopainen, J., Gregow, H., Helama, S., Kubin, E., Lummaa, V. and Terhivuo, J. 2012. History of Finnish plant phenological observations since the 1750s. *Sorbifolia*, **43**, 51–66.

Holopainen, J., Helama, S. and Väre, H. 2018. Digitizing the plant phenological dataset (1750–1875) from collections of Professor Adolf Moberg: towards the development of historical climate records. *Agricultural and Forest Meteorology*, **253−254**, 141–150. https://doi.org/10.1016/j.agrformet.2018.02.006

Holopainen, J., Helama, S. and Väre, H. 2023a. Plant phenological dataset collated by the Finnish Society of Sciences and Letters. *Ecology*, **104**(2), e3962. http://doi.org/10.1002/ecy.3962

Holopainen, J., Helama, S. and Väre, H. 2023b. The written history of plant phenology: shaping primary sources for secondary publications. *The Science of Nature – Naturwissenschaften*, **110**, 34. http://doi.org/10.1007/s00114-023-01861-w

Irannezhad, M., Chen, D. and Kløve, B. 2015. Interannual variations and trends in surface air temperature in Finland in relation to atmospheric circulation patterns, 1961–2011. *International Journal of Climatology*, **35**(10), 3078–3092. https://doi.org/10.1002/joc.4193

Jones, P. D. and Lister, D. H. 2002. The daily temperature record for St. Petersburg (1743–1996). *Climatic Change*, **53**, 253–267. https://doi.org/10.1023/A:1014918808741

Karanitsch-Ackerl, S., Mayer, K., Gauster, T., Laaha, G., Holawe, F., Wimmer, R. and Grabner, M. 2019. A 400-year reconstruction of spring–summer precipitation and summer low flow from regional tree-ring chronologies in north-eastern Austria. *Journal of Hydrology*, **577**, 123986. https://doi.org/10.1016/j.jhydrol.2019.123986

Kington, J. A. 1974. An application of phenological data to historical climatology. *Weather*, **29**(9), 320–328. https://doi.org/10.1002/j.1477-8696.1974.tb03318.x

Laaksonen, K. 1976. The dependence of mean air temperatures upon latitude and altitude in Fennoscandia (1921–1950). *Annales Academiae Scientiarum Fennicae. Series A, III. Geologica-Geographica*, **119**, 5–19.

Lappalainen, M. 2001. *Suomen kansallispuistot: ulapalta paljakalle* (*Finland's National Parks: Seas of Blue, Seas of Green*). Metsähallitus, Vantaa.

Li, J. S., Hamann, A. and Beaubien, E. 2020. Outlier detection methods to improve the quality of citizen science data. *International Journal of Biometeorology*, **64**, 1825–1833. https://doi.org/10.1007/s00484-020-01968-z

Linderholm, H. W., Björklund, J. A., Seftigen, K., Gunnarson, B. E., Grudd, H., Jeong, J.-H. et al. 2010. Dendroclimatology in Fennoscandia – from past accomplishments to future potential. *Climate of the Past*, **6**(1), 93–114. https://doi.org/10.5194/cp-6-93-2010

Linderholm, H. W., Björklund, J., Seftigen, K., Gunnarson, B. E. and Fuentes, M. 2014. Fennoscandia revisited: a spatially improved tree-ring reconstruction of summer temperatures for the last 900 years. *Climate Dynamics*, **45**, 933–947. http://dx.doi.org/10.1007/s00382-014-2328-9

Macias-Fauria, M., Grinsted, A., Helama, S. and Holopainen, J. 2012. Persistence matters: estimation of the statistical significance of paleoclimatic reconstruction statistics from autocorrelated time series. *Dendrochronologia*, **30**(2), 179–187. https://doi.org/10.1016/j.dendro.2011.08.003

Mann, M. E. 2002. The value of multiple proxies. *Science*, **297**(5586), 1481–1482. https://doi.org/10.1126/science.1074318

Mann, M. E., Zhang, Z., Rutherford, S., Bradley, R. S., Hughes, M. K., Shindell, D. et al. 2009. Global signatures and dynamical origins of the Little Ice Age and Medieval Climate Anomaly. *Science*, **326**(5957), 1256–1260. https://doi.org/10.1126/science.1177303

Matskovsky, V. V. and Helama, S. 2014. Testing long-term summer temperature reconstruction based on maximum density chronologies obtained by reanalysis of tree-ring data sets from northernmost Sweden and Finland. *Climate of the Past*, **10**(4), 1473–1487. https://doi.org/10.5194/cp-10-1473-2014

Matthews, J. A. and Briffa, K. R. 2005. The 'Little Ice Age': re-evaluation of an evolving concept. *Geografiska Annaler: Series A, Physical Geography*, **87**(1), 17–36. https://doi.org/10.1111/j.0435-3676.2005.00242.x

McCarroll, D., Loader, N. J., Jalkanen, R., Gagen, M. H., Grudd, H., Gunnarson, B. E. et al. 2013. A 1200-year multiproxy record of tree growth and summer temperature at the northern pine forest limit of Europe. *The Holocene*, **23**(4), 471–484. https://doi.org/10.1177/0959683612467483

McDermott, F., Mattey, D. P. and Hawkesworth, C. 2001. Centennial-scale Holocene climate variability revealed by a high-resolution speleothem $\delta^{18}O$ record from SW Ireland. *Science*, **294**(5545), 1328–1331. https://doi.org/10.1126/science.1063678

Melvin T. M. and Briffa K. R. 2008. A "signal-free" approach to dendroclimatic standardisation. *Dendrochronologia*, **26**(2), 71–86. https://doi.org/10.1016/j.dendro.2007.12.001

Melvin, T. M., Grudd, H. and Briffa, K. R. 2013. Potential bias in 'updating' tree-ring chronologies using regional curve standardisation: re-processing 1500 years of Torneträsk density and ring-width data. *The Holocene*, **23**(3), 364–373. https://doi.org/10.1177/0959683612460791

Mikkonen, S., Laine, M., Mäkelä, H. M., Gregow, H., Tuomenvirta, H., Lahtinen M. and Laaksonen, A. 2015. Trends in the average temperature in Finland, 1847–2013. *Stochastic Environmental Research and Risk Assessment*, **29**, 1521–1529. https://doi.org/10.1007/s00477-014-0992-2

Monserud, R. A. and Marshall, J. D. 2001. Time-series analysis of $\delta^{13}C$ from tree rings. I. Time trends and autocorrelation. *Tree Physiology*, **21**(15), 1087–1102. https://doi.org/10.1093/treephys/21.15.1087

Osborn, T. J., Briffa, K. R. and Jones, P. D. 1997. Adjusting variance for sample-size in tree-ring chronologies and other regional-mean timeseries. *Dendrochronologia*, **15**, 89–99.

Osborn, T. J., Jones, P. D., Lister, D. H., Morice, C. P., Simpson, I. R., Winn, J. P. et al. 2021. Land surface air temperature variations across the globe updated to 2019: the CRUTEM5 data set. *Journal of Geophysical Research: Atmospheres*, **126**(2), e2019JD032352. https://doi.org/10.1029/2019JD032352

Peltola, H., Kilpeläinen, A., Sauvala, K., Räisänen, T. and Ikonen, V.-P. 2007. Effects of early thinning regime and tree status on the radial growth and wood density of Scots pine. *Silva Fennica*, **41**(3), 285. http://dx.doi.org/10.14214/sf.285

Rohde, R. A. and Hausfather, Z. 2020. The Berkeley Earth land/ocean temperature record. *Earth System Science Data*, **12**(4), 3469–3479. https://doi.org/10.5194/essd-12-3469-2020

Sagarin, R. 2001. False estimates of the advance of spring. *Nature*, **414**, 600. https://doi.org/10.1038/414600a

Sagarin, R. 2009. Using nature's clock to measure phenology. *Frontiers in Ecology and the Environment*, **7**(6), 296. https://doi.org/10.1890/09.WB.020

Sagarin, R. and Micheli, F. 2001. Climate change in nontraditional data sets. *Science*, **294**(5543), 811. https://doi.org/10.1126/science.1064218

Schweingruber, F. H., Fritts, H. C., Braker, O. U., Drew, L. G. and Schär, E. 1978. The X-ray technique as applied to dendroclimatology. *Tree-Ring Bulletin*, **38**, 61–91.

Schweingruber, F. H., Bräker, O. U. and Schär, E. 1987. Temperature information from a European dendroclimatological sampling network. *Dendrochronologia*, **5**, 9–33.

Schweingruber, F. H., Briffa, K. R. and Jones, P. D. 1991. Yearly maps of summer temperatures in western Europe from A.D. 1750 to 1975 and western North America from 1600 to 1982: results of a radiodensitometrical study on tree rings. *Vegetatio*, **92**, 5–71. https://doi.org/10.1007/BF00047132

Speer, J. H. 2010. *Fundamentals of Tree-ring Research*. The University of Arizona Press, Tucson.

Tarand, A. and Kuiv, P. 1994. The beginning of the rye harvest – a proxy indicator of summer climate in the Baltic Area. In *Climatic Trends and Anomalies in Europe 1675–1715: High Resolution Spatio-temporal Reconstructions from Direct Meteorological Observations and Proxy Data – Methods and Results* (Frenzel, B., Pfister, C. and Gläser, B., eds). Gustav Fischer, Stuttgart, 61–72.

Tarand, A. and Nordli, P. Ø. 2001. The Tallinn temperature series reconstructed back half a millennium by use of proxy data. *Climatic Change*, **48**, 189–199. https://doi.org/10.1023/A:1005673628980

Tietäväinen, H., Tuomenvirta, H. and Venäläinen, A. 2010. Annual and seasonal mean temperatures in Finland during the last 160 years based on gridded temperature data. *International Journal of Climatology*, **30**(15), 2247–2256. https://doi.org/10.1002/joc.2046

Tuomenvirta, H. 2004. *Reliable estimation of climatic variations in Finland*. Dissertation. University of Helsinki, Finland.

Virkkala, R., Korhonen, K. T., Haapanen, R. and Aapala, K. 2000. Protected forests and mires in forest and mire vegetation zones in Finland based on the 8th National Forest Inventory. *The Finnish Environment*, **395**, 1–49.

Wilson, R., Anchukaitis, K., Briffa, K. R., Büntgen, U., Cook, E., D'Arrigo, R. et al. 2016. Last millennium northern hemisphere summer temperatures from tree rings: part I: the long term context. *Quaternary Science Reviews*, **134**, 1–18. https://doi.org/10.1016/j.quascirev.2015.12.005

Zhang, P., Linderholm, H. W., Gunnarson, B. E., Björklund, J. and Chen, D. 2016. 1200 years of warm-season temperature variability in central Scandinavia inferred from tree-ring density. *Climate of the Past*, **12**(6), 1297–1312. https://doi.org/10.5194/cp-12-1297-2016

Zheng, J., Hua, Z., Liu, Y. and Hao, Z. 2015. Temperature changes derived from phenological and natural evidence in South Central China from 1850 to 2008. *Climate of the Past*, **11**(11), 1553–1561. https://doi.org/10.5194/cp-11-1553-2015